Extreme Events Representation in CMCC-CM2 High and Very-High Resolution General Circulation Models

Enrico Scoccimarro[1], Daniele Peano[1], Silvio Gualdi[1], Alessio Bellucci[2], Tomas Lovato[1], Pier Giuseppe Fogli[1] and Antonio Navarra[1]

[1]Fondazione Centro Euro-Mediterraneo sui Cambiamenti Climatici, Bologna, Italy
[2]Fondazione Centro Euro-Mediterraneo sui Cambiamenti Climatici, Bologna, Italy, currently at Consiglio Nazionale delle Ricerche, Istituto di Scienze dell'Atmosfera e del Clima, Bologna, Italy

Correspondence to: Enrico Scoccimarro (enrico.scoccimarro@cmcc.it)

Abstract. The recent advancements in climate modelling partially build on the improvement of horizontal resolution in different components of the simulating system. A higher resolution is expected to provide a better representation of the climate variability, and in this work we are particularly interested in the potential improvements in representing extreme events of high temperature and precipitation. The two versions of the CMCC-CM2 model used here, adopt the highest horizontal resolutions available within the last family of the global coupled climate models developed at CMCC to participate in the CMIP6 effort.

The main aim of this study is to document the ability of the CMCC-CM2 models in representing the spatial distribution of extreme events of temperature and precipitation, under the historical period, comparing model results to observations (ERA5 Reanalysis and CHIRPS observations). For a more detailed evaluation we investigate both 6 hourly and daily time series for the definition of the extreme conditions.

In terms of mean climate, the two models are able to realistically reproduce the main patterns of temperature and precipitation. The very-high resolution version (¼ degree horizontal resolution) of the atmospheric model provides better results than the high resolution one (one degree), not only in terms of means but also in terms of extreme events of temperature defined at daily and 6-hourly frequency. This is also the case of average precipitation. On the other hand the extreme precipitation is not improved by the adoption of a higher horizontal resolution.

.

1 Introduction

A climate variation can have an impact on human activities, either as direct damages, or as lost opportunities and unfortunately also as loss of human life. Extreme climate events are involved in the vast majority of the most severe episodes. For this reason it is then very relevant to investigate General Circulation Models (GCMs) ability to simulate extreme events and to understand how the changing climate is influencing their distribution, frequency and location. GCMs simulations of the present climate have been assessed in previous generations of the Coupled Model Intercomparison Projects (CMIP; Flato et al. 2013) and, more recently, for CMIP6 (Eyring et al. 2016). Within CMIP6 the High Resolution Model Intercomparison Project protocol

(HighResMIP, Haarsma et al., 2016) was designed to understand the role of the horizontal resolution. In this paper, we present an analysis based on two version of the GCM developed at CMCC (CMCC-CM, Cherchi et al., 2019), that we use for two simulations of the present climate (1950-2014) differing only for the atmospheric horizontal resolution: HR with an horizontal

35   resolution of 1 degree and VHR with a resolution of ¼ of a degree. The two models are described in detail in the next section. The difference between the results obtained with the two versions of the model allows us to evaluate the impact of the model horizontal resolution on the temporal distribution of temperature and precipitation events compared to observations. It has been shown that the horizontal resolution can affect the representation of extreme events in state-of-the-art climate models (Van Haren et al., 2015; Iles et al., 2020). Besides, Demory et al. (2020) have shown that high resolution models, when

40   implemented with a resolution similar to VHR, achieve skills comparable to state-of-the-art Regional Climate Models in reproducing precipitation distributions over Europe. However, such analyses has employed rather low frequency data, and short-duration high-intensity precipitation events can easily escape detection if high-frequency data are not used (Meredith et al. 2020, Scoccimarro et al. 2015).

In this paper we present both, a daily and a high-frequency analysis using 6-hourly data from the experiments, comparing

45   model results to data from a reanalysis data set with comparable horizontal resolution (ERA5, Hersbach et al. 2020). The importance to evaluate extreme events at the sub-daily scale resides in the importance of such events on human health and over both urban and rural environments (Wehner et al. 2021).

The work is organized as follows: Sect. 2 describes the data and the methodology adopted, Sect.3 and Sect.4 describe the evaluation of model ability in representing the distribution of temperature and precipitation events respectively and Sect. 5

50   summarises and concludes the work.

2 Data and Methodology

2.1 The numerical experiments

The CMCC general circulation has been developed in several configurations (Cherchi et al. 2019). The model uses as atmospheric component the CAM Atmospheric component (CAM4, Neale et al. 2010). We will not go in a detailed description

55   here, but since it is worthwhile to mention for our discussion on precipitation biases, the deep convection scheme is the one developed by Zhang and McFarlane (1995), modified following Ritcher and Rasch (2008) and Raymond and Blith (1986, 1992). The scheme is based on a plume ensemble approach where it is assumed that an ensemble of convective scale updrafts may exist whenever the atmosphere is conditionally unstable in the lower troposphere. Moist convection occurs only when there is convective available potential energy (CAPE) for which parcel ascent from the sub-cloud layer acts to destroy the

60   CAPE at an exponential rate using a specified adjustment time scale.

The ocean and sea-ice components are the same in HR and VHR models: a ¼ degree horizontal resolution version for both ocean (NEMO3.6, Madec & the NEMO team, 2016) and sea-ice (CICE4, Hunke & Lipscomb, 2008). The two models object of this study differ only in the horizontal resolution of their atmospheric component (CAM4) that is one degree in HR, and ¼

degree in VHR. The land model (CLM4.5, Oleson et al., 2013) is implemented with the atmospheric model grid. The basic of
65 the coupling between the different components is described in Fogli and Iovino (2014). The single components of the coupled
model are described in detail in Cherchi et al. (2019); additional studies based on CMCC GCM can be found in Scoccimarro
et al. 2017a, Scoccimarro et al 2020, Bellucci et al. 2021. No changes are applied in terms of parameterization choices - and
relative tuning parameters - moving from HR to VHR. Also, the two model versions use the same number of vertical levels in
both atmosphere (26) and ocean (50) components. The complete set of experiments run with these two models is described in
70 Haarsma et al. 2016.

2.2 Re-analyses and observations for comparison

The model performance is evaluated comparing results to the European Centre for Medium Range Weather Forecasts
(ECMWF) ERA5 re-analyses (Hersbach et al. 2020, Andersson and Thepaut, 2008), with 137 hybrid sigma/pressure (model)
levels in the vertical, and the top level at 0.01 hPa. The data used in the paper (two-meter temperature, hereafter "temperature",
75 and precipitation) can be obtained from the Copernicus Data Store (CDS) at https://cds.climate.copernicus.eu up to hourly
frequency. The horizontal resolution is close to the one of the higher (VHR) resolution model employed here (1/4 degree) and
since we aim at the characterization of different type of extreme events, we consider both 6-hourly and daily time series for
the computation of the percentiles (see 2.3) for the chosen climate parameters temporal distributions. It is important to note
that the improvement of ERA5 reanalysis with respect to the previous ERA-Interim (Dee et al. 2011) product is due not only
80 to the increased resolution but also to the addition of new integrated observation and aircraft data covering the recent decades,
assimilated by the 4D-Var algorithm. The precipitation in ERA5 is generated by both large scale parameterizations (Forbes &
Ahlgrimm, 2014; Forbes & Tompkins, 2011; Tiedtke, 1993) and a convection scheme (Bechtold et al., 2008; Hirons et al.,
2013; Tiedtke, 1989).

For a more exhaustive evaluation of the precipitation distribution, we also take advantage of the high resolution CHIRPS
85 (Climate Hazards group Infrared Precipitation with Stations) daily observational data-set. The version 2.0 of the CHIRPS
database comprises a quasi-global (50°S-50°N, 180°E-180°W) domain, at ¼ degree resolution, and 1981 to near-present
gridded precipitation daily time series. This dataset merges three types of information: global climatology, satellite estimates,
and in situ observations (Funk et al. 2015). Since the observed precipitation is not assimilated into the ERA5 reanalysis until
2009, a comparison of model precipitation with CHIRPS, in addition to the ERA5 product, is necessary.

90 ## 2.3 Methodology

The period used to compare the simulated temperature (tas) and precipitation (pr) distributions to the observations is 1950-
2014. This time is sufficiently long to capture the temporal variability at the global scale (Schindler et al. 2015). Model
averages and 99th percentile (99p hereafter) are computed on the native grid and then the results are compared to ERA5, linearly
interpolating the re-analysis (and/or CHIRPS observations) on the model grid. The grid differences are minor and therefore
95 the interpolation introduces very little differences in the fields. We denote events belonging to the 99p as "extreme events"

(Scoccimarro et al. 2016). Two seasons are considered, December to February (DJF hereafter) and June to August (JJA hereafter) representative of the boreal winter and summer, respectively.

Percentiles computed at the daily time frequency are obtained based on a sample of 5850 (*90 days x 65 years)* events, while the percentiles computed at the six-hourly time frequency are obtained based on a sample of 23400 (*90 days x 65 years x 4 six-hourly data in a day*) events. Models versus ERA5 biases are shown as differences for temperature, expressed in degree Celsius [°C], and as percentage differences for precipitation. The precipitation biases are shown only for regions where the seasonal average of precipitation is higher than 0.5 mm/d to avoid misleading percentual differences over dry domains (Scoccimarro et al. 2013). The comparison with CHIRPS precipitation data is performed at the daily frequency only for the shorter period 1981-2014, covered by this dataset, therefore the percentiles are obtained based on a sample of 3060 (*90 days x 34 years)* events.

3 Representation of extreme events of temperature

In this section modelled extreme temperature is compared to the ERA5 reanalysis. Figure 1 shows the 99th percentile of ERA5 temperature time series at the daily (left panels) or 6-hourly (right panels) frequency, for DJF (upper panels) and JJA (lower panels). Higher values for extreme events appear when focusing on the 6-hourly results, with maximum differences (up to 5 °C) along the Tropics and in particular over central America, western India and equatorial Africa during DJF (Figure 1, upper panels) and over northern Africa, Saudi Arabia and western United States during JJA (Figure 1 lower panels).

The daily based extreme temperature bias is shown in Figure 2 for the HR and VHR models in the left and right panels respectively. The large positive DJF bias shown by the HR model at the high latitudes in the Northern Hemisphere - reaching 9 °C over Alaska, northern Canada and eastern Siberia (Figure 2, upper left panel) - is significantly reduced in the VHR model (Figure 2, upper right panel). Also the positive HR DJF bias over eastern Europe is more than halved in VHR, while the DJF negative biases over northern Africa and Tibetan Plateau worsen moving to the higher resolution (Figure 2 upper panels). The positive extreme temperature bias between 30°N and 60°N shown by the HR model during JJA (Figure 2 lower panels) is partially reduced in VHR. Similarly, the 5 to 7°C positive JJA bias over the western coast of South America in HR, results halved in VHR. On the other hand the negative JJA bias of about -8°C over north-eastern Canada shown by HR model is even worse in the VHR version, where a larger portion of the domain is subject to a bias of about -9°C.

Moving to the 6-hourly based extreme events, the fraction of land affected by a positive bias higher than 5°C is more pronounced compared to the daily statistics, especially for the HR model during JJA (Figure 3). The positive bias over north western part of South America, during JJA, reaches 9°C in HR and is only partially reduced in VHR; during the same season the positive bias of the same order of magnitude over central and eastern United States is not improved by the increased resolution. Similar patterns, but less pronounced, are reflected on the averaged temperature as shown in supplemental Figure S1.

4 Representation of extreme events of precipitation

Following the same structure as in previous section, the modelled extreme precipitation is here compared to the ERA5
130 reanalysis (from Figure 4 to Figure 6) for both daily and 6-hourly statistics, and then to the CHIRPS data-set (Figure 7) for
daily statistics only. Figure 4 shows the ERA5 seasonal extreme precipitation bias for DJF (upper panels) and JJA (lower
panels) during the historical period. Left panels of Figure 4 refer to the 99th percentile computed based on daily time series,
while the right panels refer to the same percentile, but computed on 6-hourly time series. The higher extreme events magnitude
associated to the 6-hourly results (Figure 4, right panels) compared to the daily statistics (Figure 4, left panels) is visible almost
135 everywhere, but it is more pronounced over the Tropics. In fact this is where convective processes are expected, and it is well
known that convective precipitation tends to be short lived, while long-duration intense events (from 12 hours to 3 day) are
often associated to synoptic weather systems and tend to have larger spatial scales (Chan et al. 2014, Scoccimarro et al. 2015).
While reanalysis results are shown in millimeter per day (mm/day), the model biases are shown as percentage change with
respect to ERA5 reanalysis (see Section 2.3 for details). In terms of average precipitation the VHR model shows less
140 pronounced biases with respect to HR model (Figure S2). In particular, during DJF, the negative bias over northern part of
South America is reduced from -80% to less than -50%, while the positive bias over western United States, South Africa and
Australia is almost halved. During JJA, the bias tends to be less pronounced in both models, and the differences between the
two are mainly located over Peru, Bolivia and Brazil ranging from about -80% of the HR model to values closer to zero, even
positive, over a small portion of the domain in the VHR model.
145 A different behavior is found focusing on daily extreme precipitation events. No particular differences between high and low
resolution biases are found in the Northern Hemisphere, while the VHR model tends to overestimate the 99th percentile of
daily precipitation distribution in the Southern Hemisphere, in both seasons especially within the Tropics (Figure 5). Similar
patterns emerge for the 6-hourly based extreme precipitation (Figure 6), but with a less pronounced overestimate in VHR over
the Tropics, compared to HR results.
150 To corroborate our results in terms of precipitation biases, we computed the same statistics obtained from ERA5, using the
CHIRPS observational daily dataset for averages (Figure S3) and extreme events (Figure 7). The biases computed with respect
to the CHIRPS dataset are very similar to what we already described based on ERA5, but with a reduced magnitude (Figure
7 compared to Figure 5) for extreme events in both models, during JJA, along the Tropics.
The worsening of the extreme precipitation bias moving from the HR to the VHR model is also associated to a deterioration
155 of the representation of the fraction of precipitation associated to extreme events with respect to the total precipitation: Figure
S4 shows that both models reasonably well capture this metric in both seasons compared to ERA5, but the VHR model tends
to overestimate such amount over the southern Hemisphere especially during DJF, except for the Australian domain. In
particular, the strong positive bias of DJF average precipitation over Australia (up to 140%, Figure S3, higher panels) can't be
attributed to the positive (about 50%, Figure 7 upper panels) bias found for extreme events, but must be associated to a right
160 shift of the remaining part of the precipitation distribution, more pronounced for the non-extreme events. In fact, such potential

contribution of the positive bias in extreme events to the bias in the average precipitation is also partially neglected by the model tendency to halve the fraction of water attributable to extreme events over this domain, compared to the observed fraction (Figure S4).

5 Summary and conclusions

CMCC-CM2-HR4 and CMCC-CM2-VHR4 models are state-of-the-art fully coupled climate models, participating in different Model Intercomparison Projects within the 6th Coupled Model Intercomparison Project (CMIP6). CMCC-CM2-HR4 presents a horizontal resolution typical of most of the CMIP6 involved models, while CMCC-CM2-VHR4 has a horizontal resolution standard for the model involved in the High-Resolution Model Intercomparison Project (HighResMIP). In this paper we highlight the ability of the two models to represent extreme climate conditions, based on daily and 6-hourly time series, comparing temperature and precipitation modelled distributions to the observed ones. In order to have a gridded data set representative of the observed climate at the 6-hourly time frequency we used ERA5 reanalysis, and for the precipitation analysis we also reinforce our findings on the base of the CHIRPS daily observations.

On average, the highest resolution model (VHR) is better than the lower resolution model (HR) in representing average and extreme events of temperature both in terms of patterns and magnitude. This is true for daily and 6-hourly based statistics. The described differences between the computed daily and 6-hourly biases in temperature statistics are very similar for HR and VHR models. This result suggests that the horizontal resolution is not at the base of such differences. Consequently, the worsening of model biases in high frequency (6-hourly) temperature statistics derives from deficiencies of the current version of model components and parameterizations in representing high-frequency processes.

Regarding the precipitation distribution, the VHR model performs better in representing averages, but more pronounced biases appear in VHR compared to HR when focusing on extreme events, with a more evident degradation in the daily statistics compared to the 6-hourly. This latter result reduces the confidence we usually attribute to the highest horizontal resolution in modelling extreme precipitation, and is consistent with recent findings (Bador et al. 2020) suggesting that highest resolution models tend to produce more pronounced extremes than lower resolution ones and that many of them show lower skill – both in terms of intensity and spatial distribution - at higher resolution compared to their corresponding lower resolution version. This emphasizes the need to focus not only on the horizontal resolution to improve the model ability in representing the climate system, but also on physics and tuning. In particular, in the highest resolution model, object of this analysis (VHR) the tuning parameters were kept constant, moving from the HR to the VHR version, in order to be compliant with the PRIMAVERA (EU project) protocol.

The different biases, obtained based on daily and 6-hourly time frequencies, also suggest that for the setup of model physics and tuning we need to consider the event distributions at different time frequencies, to take into account the representation of the different processes responsible of the extreme conditions emerging at the different frequencies (Scoccimarro et al. 2015).

The poor performance of climate models in representing extreme precipitation is not improved in the last CMIP6 generation models, compared to the previous CMIP5 generation (Scoccimarro et al. 2020), and in this work we have shown that this is

195 even more evident moving to the highest resolution version of the CMCC-CM2 model adopted for HighResMIP, consistently with multi-model analysis performed at the same horizontal resolution (Bador et al. 2020).

Code and Data availability

The code relative to the CMCC-CM2-HR4 and the CMCC-CM2-VHR4 climate models is available on the Zenodo

200 repository (URL: https://zenodo.org/record/5499856#.YTs5Bh2xVZP, doi: 10.5281/zenodo.5499856). The data relative to the two models are available through the ESGF data portal (Scoccimarro et al. 2017b and Scoccimarro et al. 2017c, respectively). ERA5 Reanalysis are available through the Copernicus data portal (https://climate.copernicus.eu). CHIRPS observational data set is available through the data storage of the University of California in Santa Barbara (https://www.chc.ucsb.edu/data/chirps).

205

Author contribution

ES, AB and DP implemented the two model versions and run the simulations. PGF supported the implementation of the Aerosol input management routines.TL prepared the radiative forcing files and supported the model output postprocessing. ES prepared the manuscript with contributions from all co-authors.

210 **References**

Andersson E., J.N. Thépaut: ECMWF's 4D-Var data assimilation system – the genesis and ten years in operations. ECMWF Newsl, 115, pp. 8-12, 2008.

Bador, M., Boé, J., Terray, L., Alexander, L. V., Bellucci, A., Haarsma, R., Koenigk, T., Moine, M.-P., Lohmann, K.,
215 Putrasahan, D. A., Roberts, C., Roberts, M., Scoccimarro, E., Schiemann, R., Seddon, J., Senan, R., Valcke, S., Vanniere, B : Impact of higher spatial atmospheric resolution on precipitation extremes over land in global climate models. Journal of Geophysical Research: Atmospheres, doi: 10.1029/2019JD032184, 2020.

Bechtold, P., Koehler, M., Jung, T., Doblas-Reyes, F., Leutbecher, M., Rodwell, M. J., Vitart, F., & Balsamo, G. : Advances
220 in simulating atmospheric variability with the ECMWF model: From synoptic to decadal time-scales. Quarterly Journal of the Royal Meteorological Society: A journal of the atmospheric sciences, applied meteorology and physical oceanography, 134(634), 1337–1351, 2008.

Bellucci, A., Athanasiadis, P., Scoccimarro, E. *et al.*: Air-Sea interaction over the Gulf Stream in an ensemble of HighResMIP
225   present climate simulations. *Clim Dyn*. https://doi.org/10.1007/s00382-020-05573-z, 2021.

Chan S. C., Kendon E. J., Fowler H. J., Blenkinsop S., Roberts N. M. and Ferro C. A. T. : The Value of High-Resolution Met
Office Regional Climate Models in the Simulation of Multihourly Precipitation Extremes J. Clim., 27 6155–74, 2014

230   Cherchi A., T. Lovato, P.G. Fogli, D. Peano, S. Gualdi, S. Masina, E. Scoccimarro, S. Materia, D. Iovino, and A. Navarra:
Global mean climate and main patterns of variability in the CMCC-CM2 coupled model. Journal of Advances in Modeling
Earth Systems. Doi:10.1029/2018MS001369, 2019.

Dee, D. P. *et al*.: The ERA-Interim reanalysis: configuration and performance of the data assimilation system. *Quarterly
235   Journal of the Royal Meteorological Society* 137, 553–597, 2011.

Demory, M.-E., *et al*.: European daily precipitation according to EURO-CORDEX regional climate models (RCMs) and high-
resolution global climate models (GCMs) from the High-Resolution Model Intercomparison Project (HighResMIP), Geosci.
Model Dev., 13, 5485–5506, https://doi.org/10.5194/gmd-13-5485-2020, 2020.
240
Eyring, V., S. Bony, G. A. Meehl, C. Senior, B. Stevens, R. J. Stouffer, and K. E. Taylor: Overview of the Coupled Model
Intercomparison Project Phase 6 (CMIP6) experimental design and organisation. Geosci. Model Dev. Discuss., 8, 10 539–10
583, https://doi.org/10.5194/gmdd-8-10539-2015, 2016

245   Flato, G., Marotzke, J., Abiodun, B., Braconnot, P., Chou, S. C., Collins, W., et al.: Evaluation of climate models. Climate
change 2013: The physical science basis. Contribution of Working Group I to the Fifth Assessment Report of the
Intergovernmental Panel on Climate Change, 741–866, 2013.

Forbes, R., & Ahlgrimm, M.: On the representation of high-latitude boundary layer mixed-phase cloud in the ECMWF global
250   model. Monthly Weather Review, 142(9), 3425–3445, 2014.

Forbes, R., & Tompkins, A.: An improved representation of cloud and precipitation. ECMWF Newsletter, 129, 13–18, 2011.

Funk, C., Peterson, P., Landsfeld, M. *et al.* The climate hazards infrared precipitation with stations—a new environmental
255   record for monitoring extremes. *Sci Data* **2,** 150066. https://doi.org/10.1038/sdata.2015.66, 2015.

Fogli P.G., Iovino D.: CMCC-CESM-NEMO: toward the new CMCC Earth System Model. CMCC Research Papers RP0248, 2014

260   Haarsma, R. J., and Coauthors : High Resolution Model Intercomparison Project (HighResMIP). Geosci. Model Dev., 9, 4185–4208, https://doi.org/10.5194/gmd-9-4185-2016, 2016.

Hersbach, H, Bell, B, Berrisford, P, et al.: The ERA5 global reanalysis. *Q J R Meteorol Soc*. 146: 1999– 2049. https://doi.org/10.1002/qj.3803, 2020.

265

Hirons, L., Inness, P., Vitart, F., & Bechtold, P.: Understanding advances in the simulation of intraseasonal variability in the ECMWF model. part II: The application of process-based diagnostics. Quarterly Journal of the Royal Meteorological Society, 139(675), 1427–1444, 2013.

270   Hunke, E., & Lipscomb, W.: CICE: The Los Alamos sea ice model, documentation and software, version 4.0. Los Alamos National Laboratory, Technical Report LA-CC-06-012, 2008.

Iles, C. E., Vautard, R., Strachan, J., Joussaume, S., Eggen, B. R., and Hewitt, C. D.: The benefits of increasing resolution in global and regional climate simulations for European climate extremes, Geosci. Model Dev., 13, 5583–5607,
275   https://doi.org/10.5194/gmd-13-5583-2020, 2020.

Madec, G., & the NEMO team: NEMO ocean engine—Version 3.6. Tech Rep ISSN 1288–1619 No 27 Pôle de Modélisation, Institut Pierre- Simon Laplace (IPSL), France, 2016.

280   Meredith E.P., et al.: Subhourly rainfall in a convection-permitting model Environ. Res. Lett. 15 034031, 2020.

Neale, R. B., and Coauthors,: Description of the NCAR Community Atmosphere Model (CAM4.0). NCAR Tech. Note NCAR/TN-4851STR, 212 pp, 2010.

285   Oleson, K. W., Lawrence, D. M., Bonan, G. B., Drewniak, B., Huang, M., Koven, C. D., et al.: Technical description of version 4.5 of the Community Land Model (CLM). NCAR Technical Note, NCAR/TN-503+STR, 2013.

Raymond, D. J., and A. M. Blyth,: A stochastic mixing model for non-precipitating cumulus clouds, J. Atmos. Sci., 43, 2708– 2718, 1986.

290

Raymond, D. J., and A. M. Blyth: Extension of the stochastic mixing model to cumulonimbus clouds, J. Atmos. Sci., 49, 1968–1983, 1992.

Richter, J. H., and P. J. Rasch: Effects of convective momentum transport on the atmospheric circulation in the community
295   atmosphere model, version 3, J. Climate, 21, 1487–1499, 2008.

Schindler A., A Toreti, M. Zampieri, E. Scoccimarro; S. Gualdi; S. Fukutome; E. Xoplaki; J. Luterbacher: On the internal variability of simulated daily precipitation. Journal of Climate, doi: 10.1175/JCLI-D-14-00745.1, 2015.

300   Scoccimarro E., S. Gualdi, A. Bellucci, M. Zampieri, A. Navarra: Heavy precipitation events in a warmer climate: results from CMIP5 models. Journal of Climate, DOI: 10.1175/JCLI-D-12-00850.1, 2013.

Scoccimarro E., G. Villarini, M.Vichi, M. Zampieri, P.G. Fogli, A.Bellucci, S. Gualdi: Projected changes in intense precipitation over Europe at the daily and sub-daily time scales. *Journal of Climate, doi: 10.1175/JCLI-D-14-00779.1*, 2015.
305
Scoccimarro E., S. Gualdi, A. Bellucci, M. Zampieri, A. Navarra: Heavy precipitation events over the Euro-Mediterranean region in a warmer climate: results from CMIP5 models. *Regional Environmental Change*, doi:10.1007/s10113-014-0712-y, 2016.

310   Scoccimarro E., P.G. Fogli. K. Reed, S. Gualdi, S.Masina, A. Navarra: Tropical cyclone interaction with the ocean: the role of high frequency (sub-daily) coupled processes. *Journal of Climate*, doi: 10.1175/JCLI-D-16-0292.1, 2017a.

Scoccimarro E., A. Bellucci, D. Peano: CMCC CMCC-CM2-HR4 model output prepared for CMIP6 HighResMIP hist-1950. Earth System Grid Federation, https:// doi.org/10.22033/ESGF/CMIP6.1359, 2017b.
315
Scoccimarro E., A. Bellucci, D. Peano: CMCC CMCC-CM2-VHR4 model output prepared for CMIP6 HighResMIP. Earth System Grid Federation, https://doi.org/10.22033/ ESGF/CMIP6.1367, 2017c.

Scoccimarro E., Gualdi S., Bellucci A. , Peano D., Cherchi A., Vecchi G.A. , Navarra A.: The typhoon-induced drying of the
320   Maritime Continent. PNAS doi: 10.1073/pnas.1915364117, 2020.

Scoccimarro E., Gualdi S.: Heavy Daily Precipitation Events in the CMIP6 Worst-Case Scenario: Projected Twenty-First-Century Changes. Journal of Climate, doi: 10.1175/JCLI-D-19-0940.1, 2020.

325 Tiedtke, M.: Representation of clouds in large-scale models. Monthly Weather Review, 121(11), 3040–3061., 1993.

Van Haren, R., Haarsma, R. J., de Vries, H., van Oldenborgh, G. J.,and Hazeleger, W.: Resolution dependence of circulation forcedfuture central European summer drying, Environ. Res. Lett., 10,055002, doi:10.1088/1748-9326/10/5/055002, 2015.

330 Wehner M., Lee J., Risser M., Ullrich P., Gleckler P., and Collins W. D.: Evaluation of extreme sub-daily precipitation in high-resolution global climate model simulationsPhil. Trans. R. Soc. A.379: 20190545.http://doi.org/10.1098/rsta.2019.0545, 2021.

Zhang, G. J., and N. A. McFarlane: Sensitivity of climate simulations to the parameterization of cumulus convection in the
335 Canadian Climate Centre general circulation model, Atmosphere-Ocean, 33, 407–446, 1995.

.
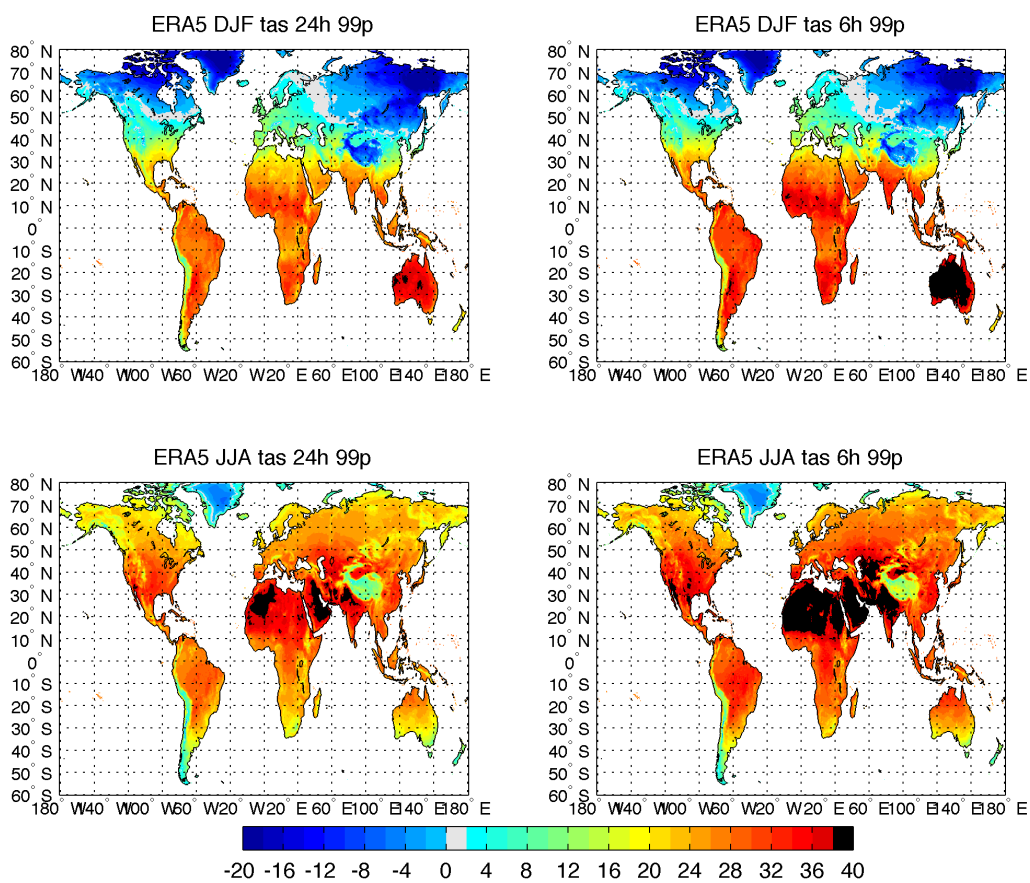
340

Figure 1: ERA5 Extreme Temperature (99th percentile, 99p). Left/Right panel shows percentiles computed based on 24h/6h time series. Upper/Lower panel shows boreal winter (DJF)/summer (JJA) results. Units are [ºC].
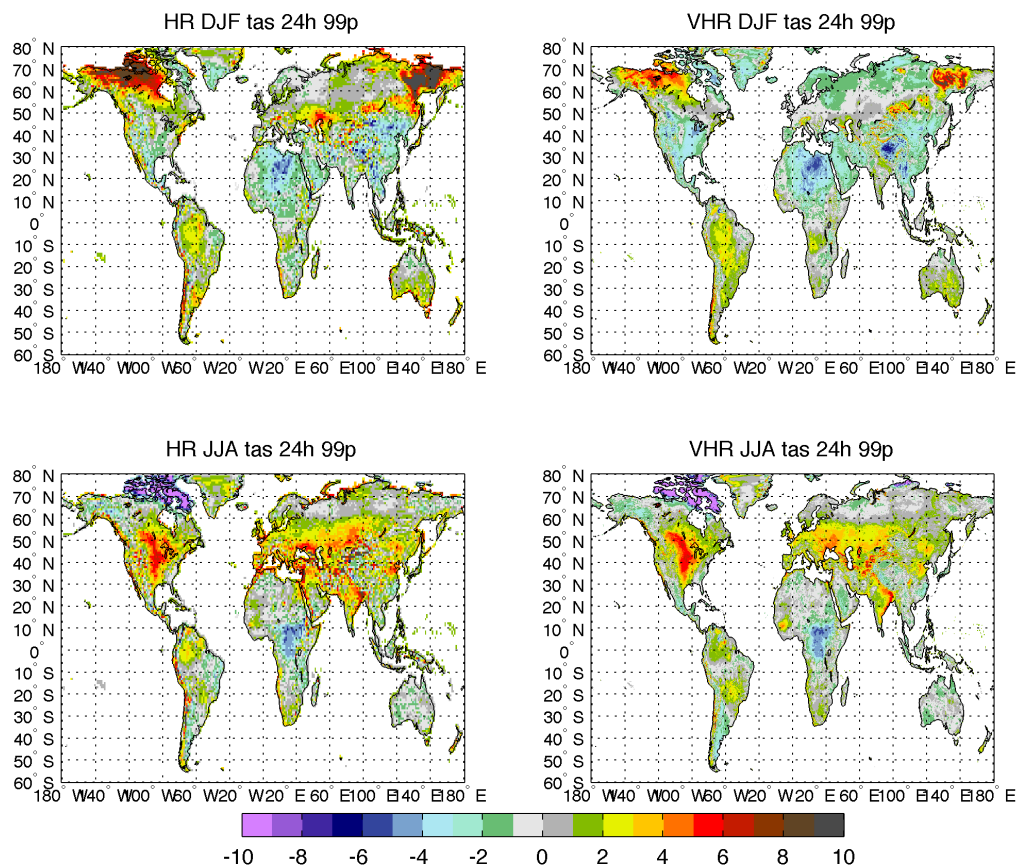
Figure 2: Daily based Extreme Temperature (99ᵗʰ percentile, 99p) bias. Left/Right panel shows HR/VHR model bias compared to ERA5. Upper/Lower panel shows boreal winter (DJF)/summer (JJA) results. Units are [ºC].
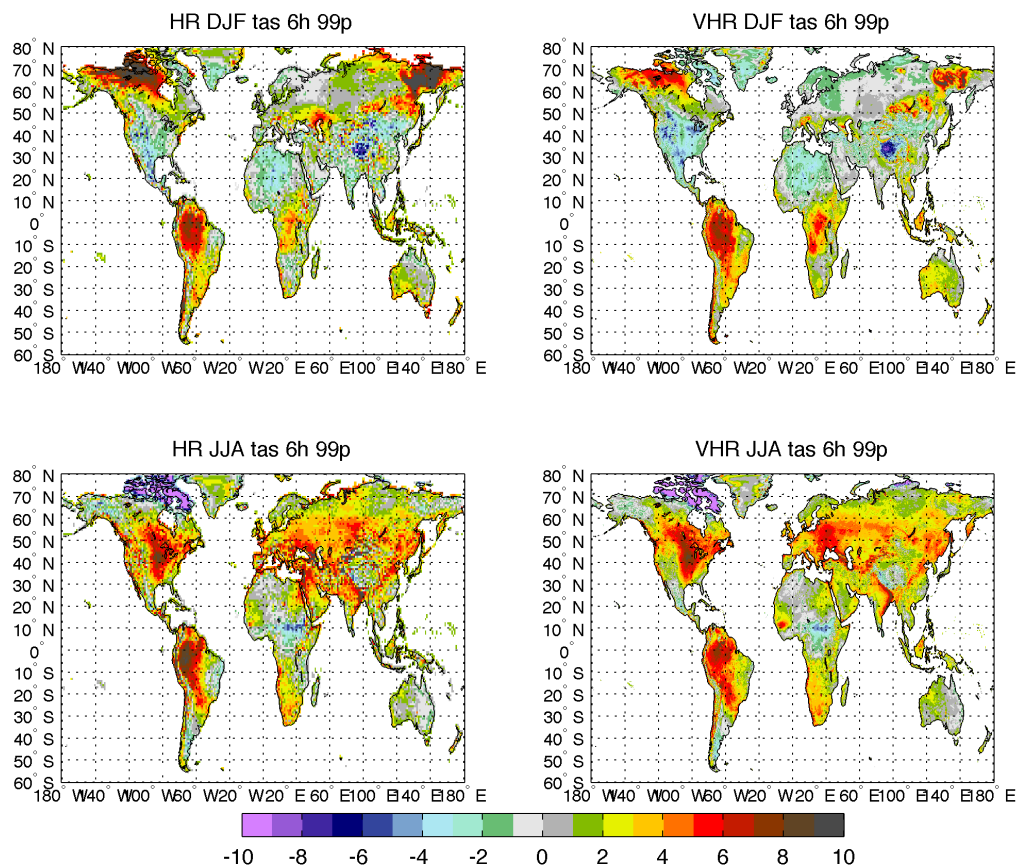
Figure 3: Six-hourly based Extreme Temperature (99ᵗʰ percentile, 99p) bias. Left/Right panel shows HR/VHR model bias compared to ERA5. Upper/Lower panel shows boreal winter (DJF)/summer (JJA) results. Units are [ºC].
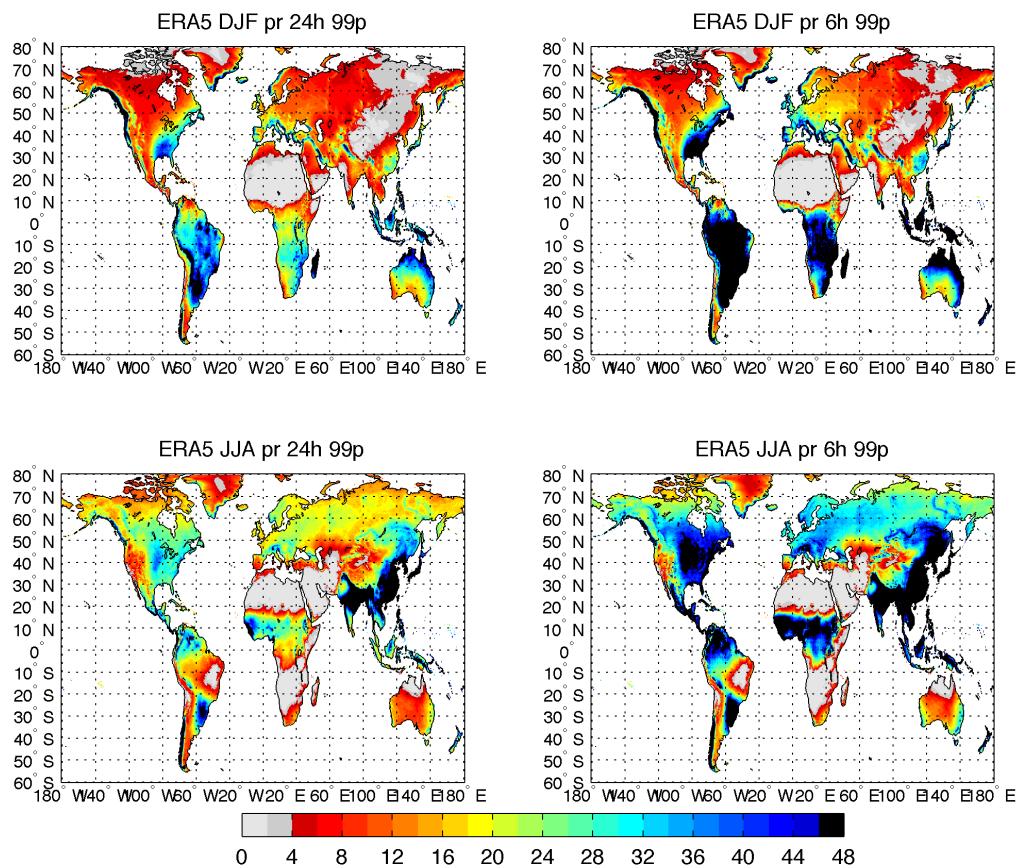
350

Figure 4: ERA5 Extreme Precipitation (99th percentile, 99p). Left/Right panel shows percentiles computed based on 24/6h time series. Upper/Lower panel shows boreal winter (DJF) /summer (JJA) results. Units are [mm/d].
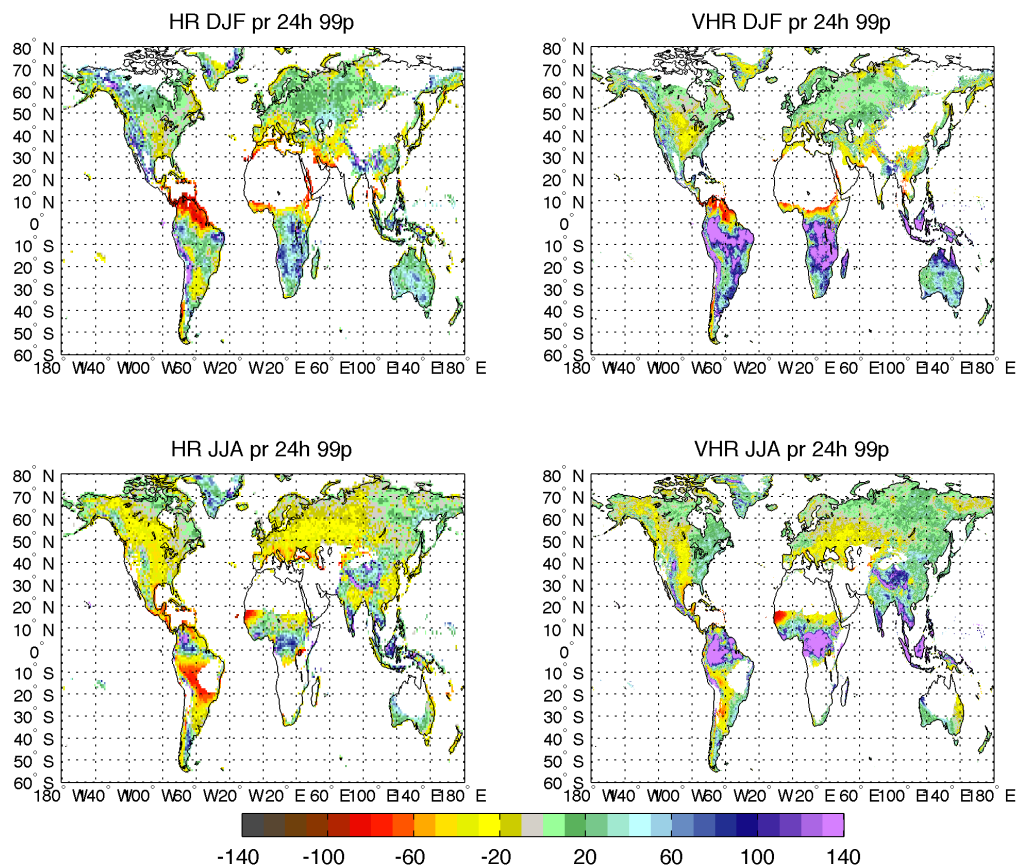
355

Figure 5: Daily based Extreme Precipitation (99th percentile, 99p) bias. Left/Right panel shows HR/VHR model bias compared to ERA5. Upper/Lower panel shows boreal winter (DJF)/summer (JJA) results. Units are [%]. White areas over land represent regions where the seasonal average precipitation is lower than 0.5 mm/d in ERA5.
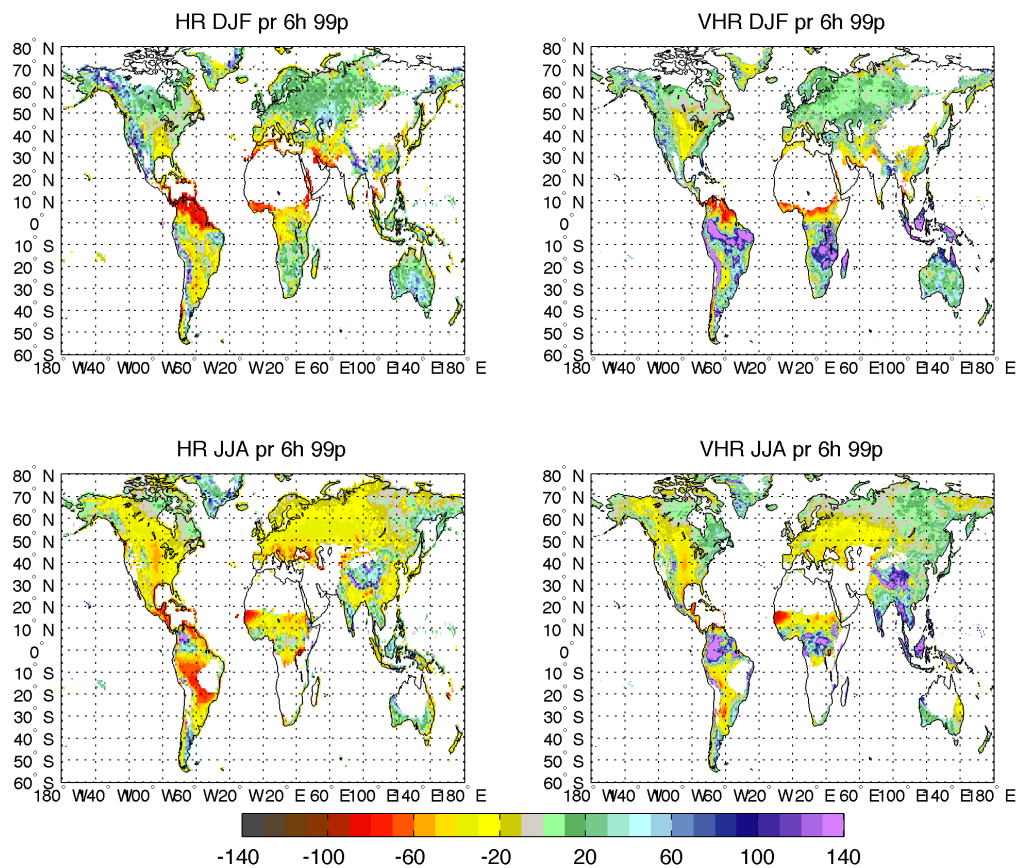
360 **Figure 6: Six-hourly based Extreme Precipitation (99th percentile, 99p) bias. Left/Right panel shows HR/VHR model bias compared to ERA5. Upper/Lower panel shows boreal winter (DJF) /summer (JJA) results. Units are [%]. White areas over land represent regions where the seasonal average precipitation is lower than 0.5 mm/d in ERA5.**
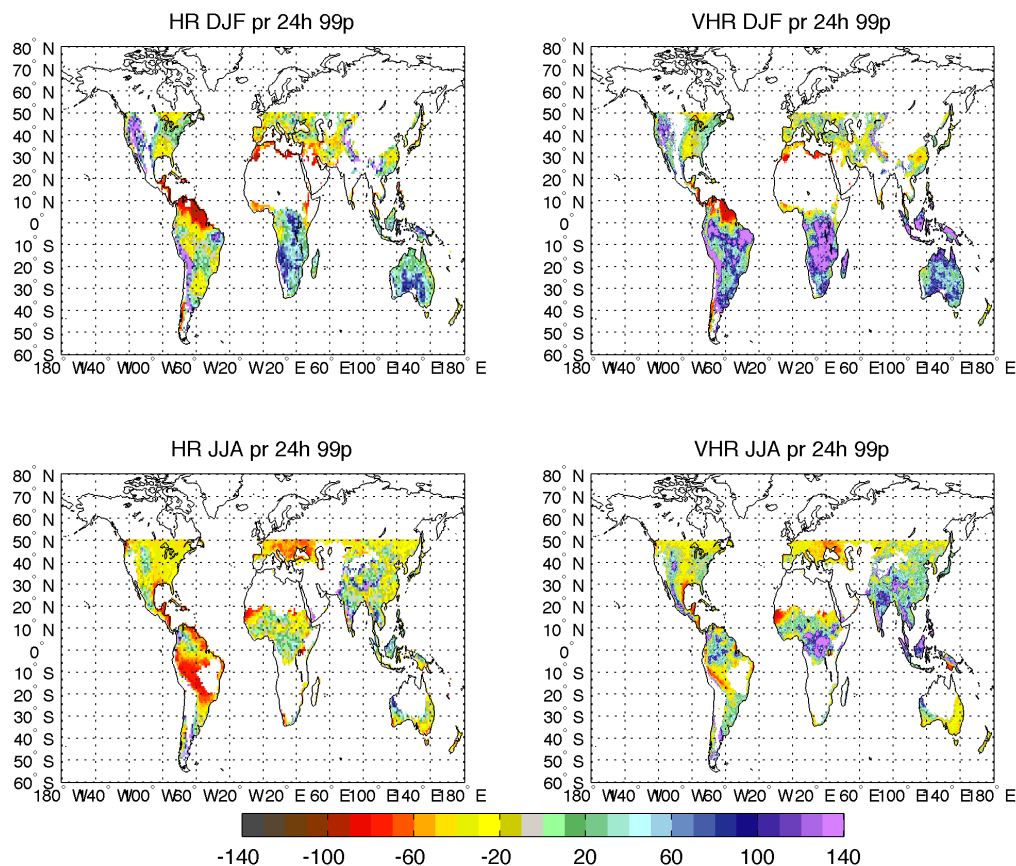
Figure 7: Same as Figure 5 but compared to CHIRPS observations instead of ERA5. Daily based Extreme Precipitation (99th percentile, 99p) bias. Left/Right panel shows HR/VHR model bias compared to CHIRPS. Upper/Lower panel shows boreal winter (DJF)/summer (JJA) results. Units are [%]. White areas over land represent regions where the seasonal average precipitation is lower than 0.5 mm/d in CHIRPS. Precipitation poleward than +-50 degrees is not available in CHIRPS data set.